Supporting Information

Polymer surface ligand and silica coating induced highly stable and enhanced aqueous fluorescent perovskite nanocrystal for efficient Hg^{2+} and glutathione detection

Yun Shu,[a] Linyan Sun,[a] Yan Wang,[a] Dangqin Jin,[b] Qin Xu,[a,*] Xiaoya Hu[a,*]

[a]*School of Chemistry and Chemical Engineering, Yangzhou University, Yangzhou 225002, P.R.China*

[b]*Department of Chemical Engineering, Yangzhou Polytechnic Institute, Yangzhou 225127, P.R.China*

[*]*Corresponding author. Email: xuqin@yzu.edu.cn, xyhu@yzu.edu.cn*

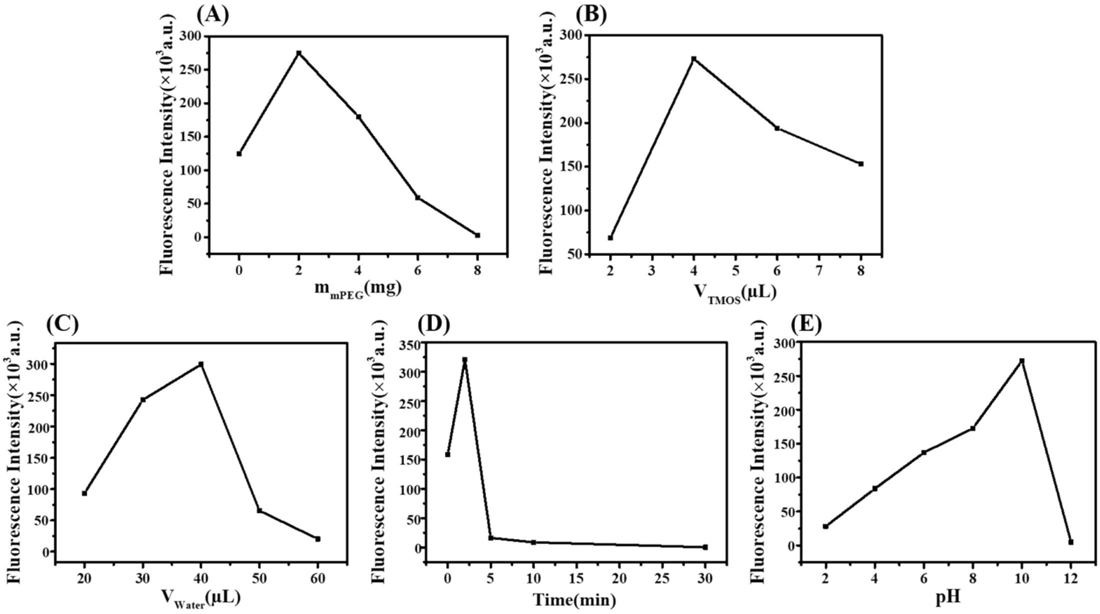

Fig. S1. Influence of different reaction conditions on fluorescence intensity of $CsPbBr_3$-mPEG@SiO_2 NCs. (A) amounts of mPEG-NH_2, (B) volume of added TMOS and (C) water. (D) Stirring time after adding water. (E) Fluorescence intensity at different pH

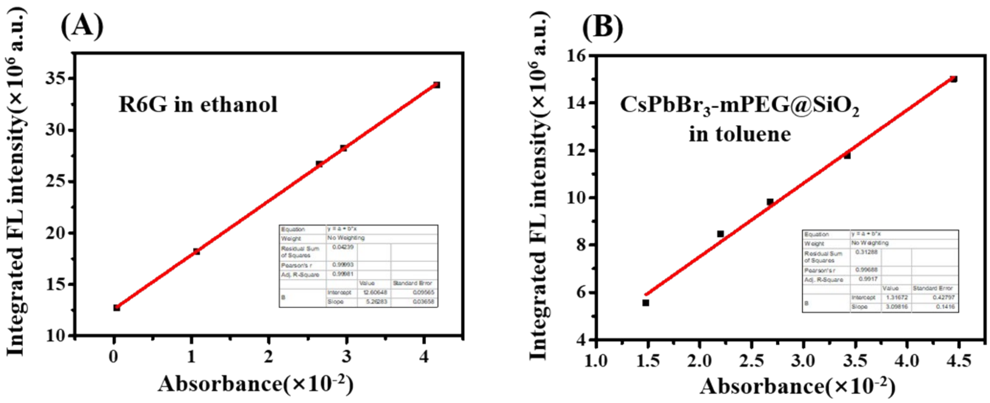

Fig. S2. The graph of Integrated FL intensity/Absorbance: (A) R6G in ethanol, (B) $CsPbBr_3$-mPEG@SiO_2 in toluene, respectively.

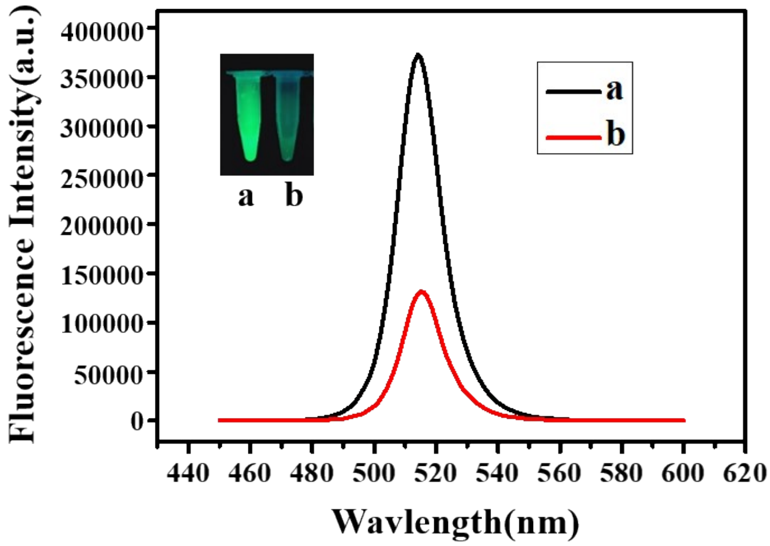

Fig. S3. Feasibility diagram of $CsPbBr_3$-mPEG@SiO_2 NCs fluorescence quenching, the illustration is the corresponding fluorescent physical picture. Fluorescence spectra of (a) $CsPbBr_3$-mPEG@SiO_2 solution and (b) $CsPbBr_3$-mPEG@SiO_2 solution with Hg^{2+}.

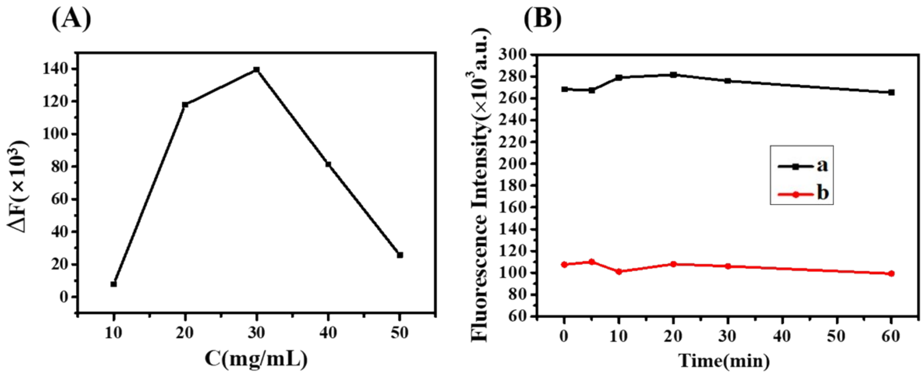

Fig. S4. (A) Changes in fluorescence quenching of $CsPbBr_3$-mPEG@SiO_2 NCs at different concentration of $CsPbBr_3$-mPEG@SiO_2. $\Delta F = F_0 - F$, where F_0 and F are the fluorescence intensity of $CsPbBr_3$-mPEG@SiO_2 solution in the absence and presence of Hg^{2+}. (B) Effect of time on the fluorescence intensity of (a) $CsPbBr_3$-mPEG@SiO_2 NCs and (b) $CsPbBr_3$-mPEG@SiO_2+Hg^{2+} (50 nM).

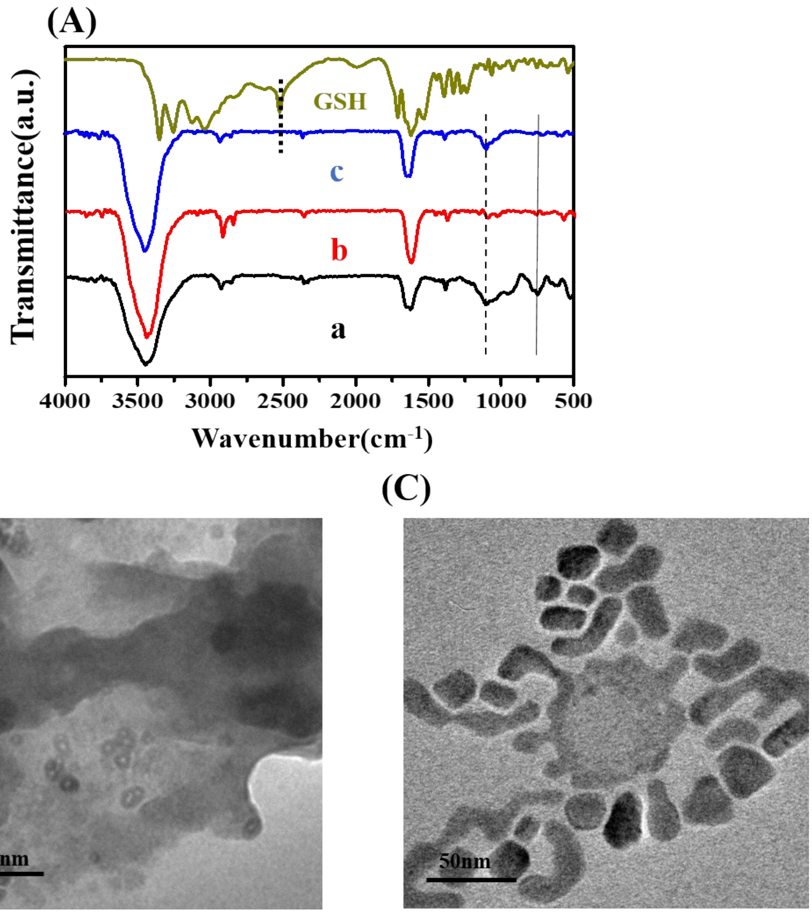

Fig. S5. (A) The FT-IR spectra of the (a) $CsPbBr_3$-mPEG@SiO_2, (b) $CsPbBr_3$-mPEG@SiO_2+Hg^{2+}, (c) $CsPbBr_3$-mPEG@SiO_2+Hg^{2+}+GSH and GSH. (B, C) TEM image of $CsPbBr_3$-mPEG@SiO_2+Hg^{2+} and $CsPbBr_3$-mPEG@SiO_2+Hg^{2+}+GSH in water solution.

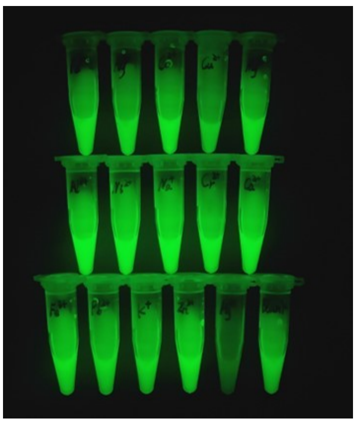

Fig. S6. Fluorescent physical map of $CsPbBr_3$-mPEG@SiO_2 in the presence of Hg^{2+} (50 nM) and other cations (50 μM), respectively.

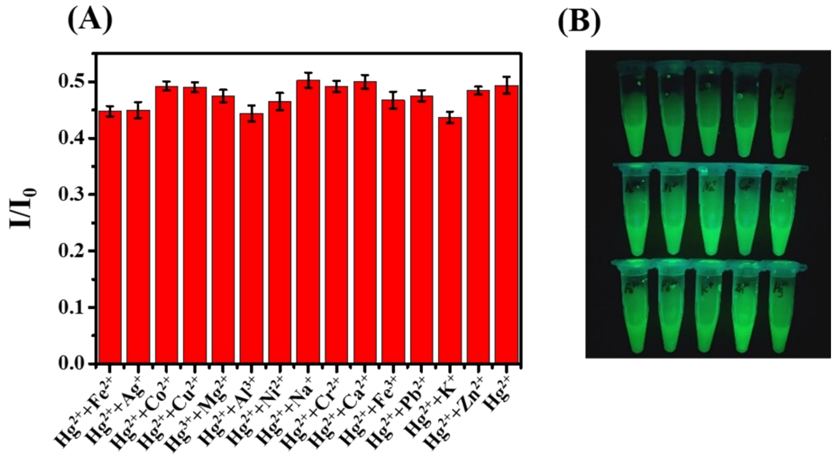

Fig. S7. (A) Change in the fluorescence intensity of $CsPbBr_3$-mPEG@SiO_2 in the presence of Hg^{2+} (50 nM) with various coexisting cations (50 μM). (B) Fluorescent physical map of $CsPbBr_3$-mPEG@SiO_2 in the presence of Hg^{2+} (50 nM) with various coexisting cations (50 μM).

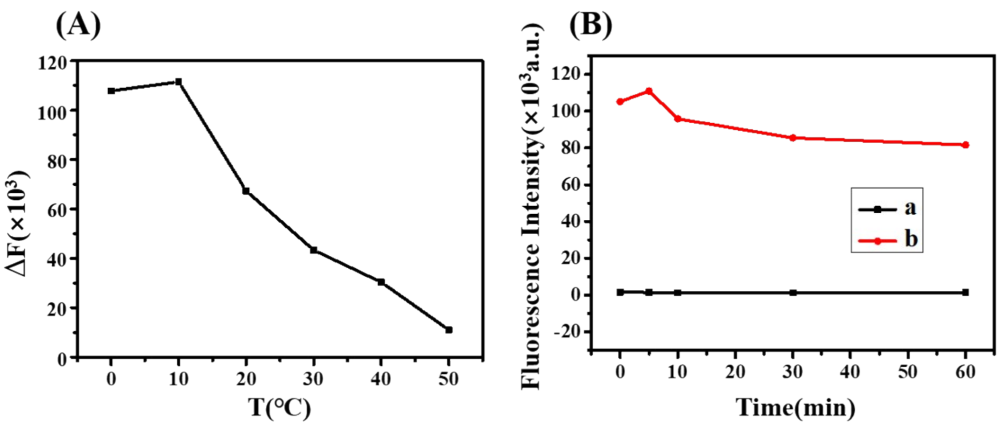

Fig. S8. (A) Changes in fluorescence quenching of $CsPbBr_3$-mPEG@SiO_2 at different T. $\Delta F = F - F_0$, where F and F_0 are the fluorescence intensity of $CsPbBr_3$-mPEG@SiO_2+Hg^{2+} in the presence and absence of GSH. (B) Effect of time on the fluorescence intensity of (a) $CsPbBr_3$-mPEG@SiO_2+Hg^{2+} and (b) $CsPbBr_3$-mPEG@SiO_2+Hg^{2+}+GSH (20 μM).

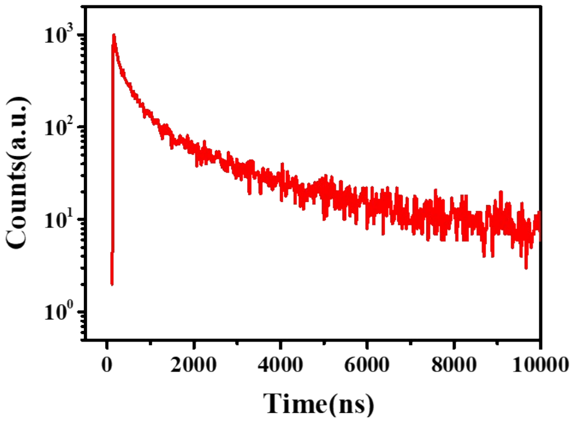

Fig. S9. Fluorescence decay curves of $CsPbBr_3$-mPEG@SiO_2 NCs with concentrations of 100 nM Hg^{2+} and 10 μM GSH

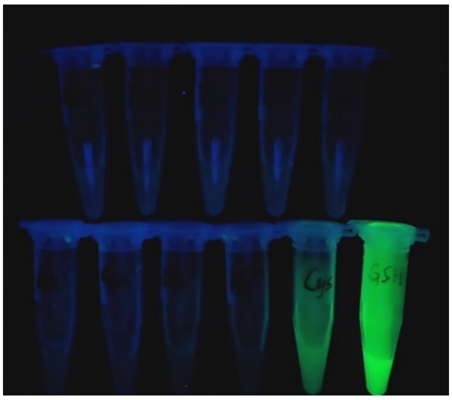

Fig. S10. Fluorescent physical map of $CsPbBr_3$-mPEG@SiO_2+Hg^{2+} in the presence of GSH (50 μM) and other small biological molecules (50 μM), respectively.

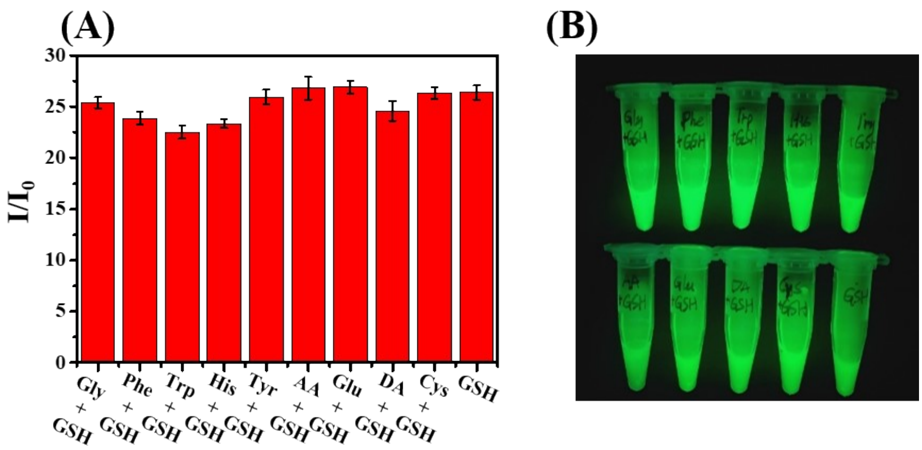

Fig. S11. (A) Change in the fluorescence intensity of $CsPbBr_3$-mPEG@SiO_2+Hg^{2+} in the presence of GSH (50 μM) with various coexisting small biological molecules (50 μM). (B) Fluorescent physical map of $CsPbBr_3$-mPEG@SiO_2+Hg^{2+} in the presence of GSH (50 μM) with various coexisting small biological molecules (50 μM).

Table S1

Comparison of different methods for Hg^{2+} detection

Fluorescent sensor	emission peak (nm)	linear range (nM)	LOD (nM)	Ref.
$CH_3NH_3PbBr_3$ QDs	520	0-100	0.124	[1]
CDs-RhB	440	500-10000	25	[2]
N QDs	515	0-20000	0.63	[3]
N-Si QDs	440	100-4000	24	[4]
Carbon dots	450	0-15000	25	[5]
SiNPs/AuNCs nanohybrid	511	20-24000	5.6	[6]
CdS/ZnS core-shell QDs	475	2.5-280	2.2	[7]
Carbon dots	399	0-4000	250	[8]
N-S CDs	450	10-250	6.5	[9]
CsPbBr3-mPEG@SiO2 NCs	520	0.1-50	0.08	This work

Table S2

The detailed recombination lifetimes of $CsPbBr_3$-mPEG@SiO_2 NCs with various concentrations of Hg^{2+}: (a) 0 nM, (b) 50 nM, (c) 100 nM, (d)the concentration of 100 nM Hg^{2+} and 10μM GSH

Time	τ_1(ns)	A_1	τ_2(ns)	A_2	τ_3(ns)	A_3	τ_{ave}(ns)
a	364.25	438.01	64.32	468.24	2535.10	90.18	1529.13
b	226.88	454.13	30.03	484.57	1787.62	75.29	929.55
c	49.76	1031.38	0.20	-80.91	518.85	94.67	252.54
d	62.34	449.11	410.94	441.04	2703.18	55.73	1651.06

Table S3

Comparison of different methods for GSH detection

Fluorescent sensor	emission peak (nm)	linear range (μM)	LOD (μM)	Ref.
N-Si QDs	440	0.1-5	0.055	[4]
CDs-RhB	440	0-10	0.02	[2]
AuNCs	600	1.99-440	0.27	[10]
AuNCs@C_{30}	445	0-0.1	0.018	[11]
BSA-AgNCs	598	10-80	1.2	[12]
AgNCs/NCDs	450/650	20-80	0.4	[13]
DNA-AgNCs	640	0.5-4.5	0.172	[14]
N-S-CD	446	0.1-2.0	0.0168	[9]
MnO_2-SiQD	464	13.3-417	0.153	[15]
$CsPbBr_3$-mPEG@SiO_2 NCs	520	1-10	0.19	This work

Table S4

Analytical results for Hg^{2+} detection in tap water samples

Sample	Spiked (nM)	Found (nM)	Recovery (%)	RSD (%, n=3)
Tap water	10	9.97	99.70	1.3
	20	20.72	103.60	0.7
	40	39.73	99.33	1.1

Table S5

Analytical results for GSH detection in human serum samples

Sample	Spiked (μM)	Found (μM)	Recovery (%)	RSD (%, n=3)
serum	0	2.92	0	0
	1	3.90	98.0	1.73
	2	4.99	103.5	3.14
	3	6.16	108.0	2.58

References

1 L. Q. Lu, T. Tan, X. K. Tian, Y. Li and P. Deng, Anal *Chim Acta,* 2017, **986**, 109-114.

2 S. Lu, D. Wu, G. Li, Z. Lv, Z. Chen, L. Chen, G. Chen, L. Xia, J. You and Y. Wu, *RSC Advances,* 2016, **6**, 103169-103177.

3 Z. Wu, M. Feng, X. Chen and X. Tang, *J Mater Chem B,* 2016, **4**, 2086-2089.

4 S. Shen, B. Huang, X. Guo and H. Wang, *J Mater Chem B,* 2019, **7**, 7033-7041.
5 Y. Ma, Z. Zhang, Y. Xu, M. Ma, B. Chen, L. Wei and L. Xiao, *Talanta,* 2016, **161**, 476-481.
6 F. Ru, P. Du and X. Lu, *Anal Chim Acta,* 2020, **1105**, 139-146.
7 M. Koneswaran and R. Narayanaswamy, *Microchimica Acta,* 2012, **178**, 171-178.
8 Z. Bai, F. Yan, J. Xu, J. Zhang, J. Wei, Y. Luo and L. Chen, *Spectrochim Acta A Mol Biomol Spectrosc,* 2018, **205**, 29-39.
9 S. Xu, Y. Liu, H. Yang, K. Zhao, J. Li and A. Deng, *Anal Chim Acta,* 2017, **964**, 150-160.
10 Y. Zhang, H. Xu, Y. Chen, X. You, Y. Pu, W. Xu and X. Liao, *J Fluoresc,* 2020, **30**, 1491-1498.
11 Z. Zhang, T. Liu, S. Wang, J. Ma, T. Zhou, F. Wang, X. Wang and G. Zhang, *J. Photochem. Photobiol. A,* 2019, **370**, 89-93.
12 Z. Chen, D. Lu, Z. Cai, C. Dong and S. Shuang, *Luminescence,* 2014, **29**, 722-727.
13 S. Zhang, B. Lin, Y. Yu, Y. Cao, M. Guo and L. Shui, *Spectrochim Acta A Mol Biomol Spectrosc,* 2018, **195**, 230-235.
14 C. Li and C. Wei, *Sens. Actuators B Chem,* 2017, **240**, 451-458.
15 H. Ma, X. Li, X. Liu, M. Deng, X. Wang, A. Iqbal, W. Liu and W. Qin, *Sens. Actuators B Chem,* 2018, **255**, 1687-1693.